research articles Journal of proteome research

Characterization of the Liver Tissue Interstitial Fluid (TIF) Proteome Indicates Potential for Application in Liver Disease Biomarker Discovery

Wei Sun,[†] Jie Ma,[†] Songfeng Wu,[†] Dong Yang,[†] Yujuan Yan,[†] Kehui Liu,[†] Jinglan Wang,[†] Longqin Sun,[†] Ning Chen,[†] Handong Wei,[†] Yunping Zhu,[†] Baocai Xing,[‡] Xiaohang Zhao,[§] Xiaohong Qian,[†] Ying Jiang,*[,†] and Fuchu He*[,†,||]

State Key Laboratory of Proteomics, Beijing Proteome Research Center, Beijing Institute of Radiation Medicine, Beijing 102206, P. R. China, Beijing Cancer Hospital, Beijing 100036, P. R. China, Cancer Institute (Hospital), Peking Union Medical College & Chinese Academy of Medical Sciences, Beijing 100021, P. R. China, and Institutes of Biomedical Sciences Fudan University, Shanghai 200032, P. R. China

Received October 12, 2009

Tissue interstitial fluid (TIF) forms the interface between circulating body fluids and intracellular fluid. Pathological alterations of liver cells could be reflected in TIF, making it a promising source of liver disease biomarkers. Mouse liver TIF was extracted, separated by SDS-PAGE, analyzed by linear ion trap mass spectrometer, and 1450 proteins were identified. These proteins may be secreted, shed from membrane vesicles, or represent cellular breakdown products. They show different profiling patterns, quantities, and possibly modification/cleavage of intracellular proteins. The high solubility and even distribution of liver TIF supports its suitability for proteome analysis. Comparison of mouse liver TIF data with liver tissue and plasma proteome data identified major proteins that might be released from liver to plasma and serve as blood biomarkers of liver origin. This result was partially supported by comparison of human liver TIF data with human liver and plasma proteome data. Paired TIFs from tumor and nontumor liver tissues of a hepatocellular carcinoma patient were analyzed and the profile of subtracted differential proteins supports the potential for biomarker discovery in TIF. This study is the first analysis of the liver TIF proteome and provides a foundation for further application of TIF in liver disease biomarker discovery.

Keywords: tissue interstitial fluid • liver • proteomics • biomarker • plasma • hepatocellular carcinoma

Introduction

The liver performs essential functions by expressing hepatocyte-specific genes, which encode plasma proteins, enzymes involved in metabolism, and proteins that participate in the detoxification of exogenous chemicals.[1] In addition to hepatocytes, which contribute roughly 80% of the liver mass, there are many types of nonparenchymal cells (NPCs), such as sinusoidal endothelial cells, Kupffer cells, hepatic stellate cells, and pit cells. Crosstalk occurs between the NPCs and hepatocytes through paracrine secretion and NPCs form the cellular microenvironment of hepatocytes. For example, hepatocyte DNA synthesis is increased by factors released from NPCs in inflammation-driven hepatocarcinogenesis.[2] Further, blood, bile, and lymph fluid form the fluid microenvironment of the hepatocytes and accommodate substances that play a role in signal exchange within the cellular microenvironment. The liver tissue interstitial fluid (TIF) is the medium between the circulating body fluids, such as plasma, and the intracellular fluid (Figure 1). Because pathological changes in liver cells could be reflected in the composition of the TIF, it could be a promising source for discovery of biomarkers of liver diseases, such as hepotocellular carcinoma (HCC), one of the most common malignant tumor types in humans. It is known that the tumor microenvironment, including premalignant cells, stromal cells, extracellular matrix components, inflammatory cells, and a range of soluble mediators, such as cytokines and growth factors, contributes to tumor development and progression.[3−7] At the same time, proteins secreted or shed from tumor cells could also exist in TIF and could prove to be useful biomarkers.

Compared with plasma, a commonly used resource for biomarker discovery, TIF has the advantage of not having the disease-associated proteins diluted in a large biofluid volume (5 L plasma in adult) or being muddled with unrelated proteins from other organs and tissues. TIF should be more promising for clinical proteomic analysis since low-abundance local

* Corresponding authors: Fuchu He, State Key Laboratory of Proteomics, Beijing Proteome Research Center, Beijing Institute of Radiation Medicine, Beijing 100850, P. R. China. Tel and fax, 8610-68177417; e-mail, hefc@nic.bmi.ac.cn. Ying Jiang, State Key Laboratory of Proteomics, Beijing Proteome Research Center, Beijing Institute of Radiation Medicine, Beijing 102206, P. R. China. Tel, 8610-80705299; fax, 8610-80705002; e-mail, jiangying304@hotmail.com.
[†] Beijing Institute of Radiation Medicine.
[‡] Beijing Cancer Hospital.
[§] Peking Union Medical College & Chinese Academy of Medical Sciences.
[||] Institutes of Biomedical Sciences Fudan University.

10.1021/pr9009172

Published on Web 12/29/2009

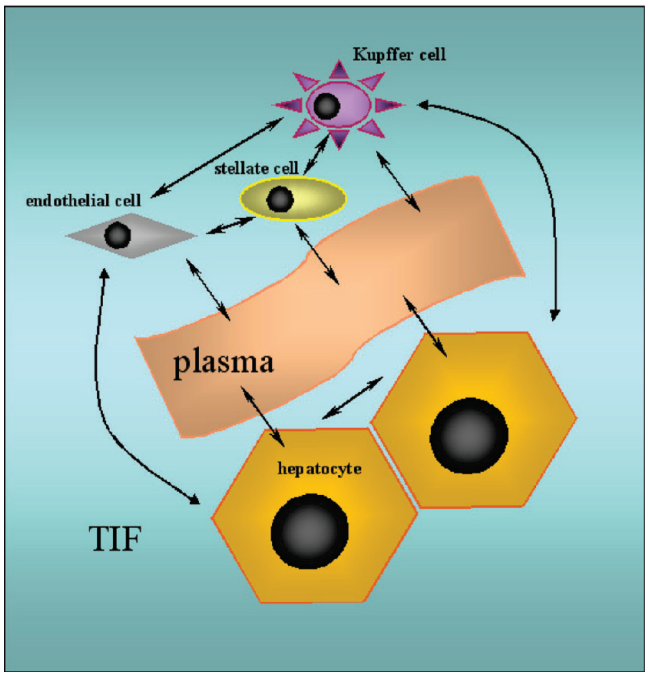

Figure 1. Schematic diagram of liver TIF as the interface between the circulating body fluids, such as plasma, and the intracellular fluid.

proteins are enriched in comparison to plasma. This theory is supported by studies showing that ovarian neoplasm- or pancreatic adenocarcinoma-associated proteins are enriched in cystic fluid[8] and pancreatic juice[9] compared with their levels in serum. In summary, the association of TIF with disease proteins is relatively direct compared with that of plasma/serum (Supporting Information Table S1).

In biomarker discovery research, plasma/serum is an obvious choice because of its accessibility and usefulness in clinical application. Most major categories of protein in the human proteome are represented in plasma. The human plasma proteome project (HPPP) nonredundant list confirms the presence of a number of interesting candidate marker proteins in plasma and serum.[10] Many kinds of quantitative proteomics techniques have been applied to biomarker discovery in plasma/serum, from gel-based to nongel-based ones, including two-dimensional gel electrophoresis, cICAT (cleavable isotope-coded affinity tag), iTRAQ (isobaric tag for relative and absolute quantitation), SELDI (surface enhanced laser desorption ionization), MELDI (material enhanced laser desorption ionization), and so on. HPPP and other groups have devoted a great deal of effort to technical improvements, such as high-abundance protein depletion, prefractionation, and repeat analysis. Although the complexity of the plasma proteome remains a challenge, successful studies have been carried out, as in the case of pancreatic tumors.[11] Tissue-based proteomic studies have also been carried out for biomarker discovery. However, only those differentially expressed proteins that are secreted into body fluids have the potential for clinical application.

On the basis of this concept, in addition to plasma/serum and tissue, proximal fluids have emerged as a novel source for biomarker discovery. Notably, Celis and co-workers have profiled the TIF proteome of human breast carcinoma, making a significant contribution to the current body of knowledge in this field.[12,13] However, the absence of cellular protein contamination in TIF has not been demonstrated; such an analysis is critical for determining the appropriate method for extraction of TIF and for data annotation. We evaluated the contamination of TIF extracted from liver tissue and displayed its characteristic by proteomic method. The protein flow from liver to plasma via TIF was analyzed and the result suggested that certain kinds of proteins are released from liver to plasma and serve as blood biomarkers of liver origin. We then conducted subtractive proteomic analysis on paired tumor and nontumor liver TIFs from a HCC patient. The reported association of high-confidence unique proteins in HCC TIF indicated the promising potential of TIF in biomarker discovery. This is the first proteomic analysis of liver TIF and the first evaluation of the application of liver TIF in HCC biomarker discovery.

Experimental Procedures

Reagents. Immobiline DryStrip gels (24 cm, pH 3−10), Pharmalyte (pH 3−10), Cy2, Cy3, and Cy5 were purchased from GE Healthcare (Piscataway, NJ). Dimethylformamide (DMF) was purchased from Aldrich (99.8%, Steinheim, Germany). Dithiothreitol (DTT), urea, agarose, glycerol, bromophenol blue, 3-[(3-Cholamidopropyl) dimethylammonio] propanesulfonic acid (CHAPS), mineral oil, acrylamide, Bis, trihydroxymethylaminomethane (Tris), glycine, sodium dodecyl sulfate (SDS), and iodoacetamide were purchased from Bio-Rad (electrophoresis purity reagent, Hercules, CA). Thiourea was purchased from Fluka (>99%, Buchs, Switzerland). Protease inhibitor cocktail was purchased from Roche (Penzberg, Germany). Trypsin (sequencing grade) was purchased from Promega (Madison, WI). Acetonitrile (ACN) was purchased from Fisher (Fair Lawn, NJ). Trifluoroacetic acid (TFA) was purchased from Merck (Schuchardt, Hohenbrunn, Germany). ACN and TFA were high performance liquid chromatography (HPLC) grade. Other commonly used chemicals were analytical grade. All buffers were prepared with Milli-Q water (Millipore, Bedford, MA).

Sample Collection. C57BJ/6 L mice were sacrificed for liver TIF extraction. The adjacent normal human liver tissue was obtained from a patient undergoing hemangioma surgery. Extensive clinical data were collected after obtaining informed consent. Donors with evidence of viral hepatitis, autoimmune liver disease, cystic liver disease, fatty liver disease, or other liver disease were excluded. The results of imaging (B-type ultrasound) and tissue histopathologic examination of the resected liver were normal. Paired tumor and nontumor liver tissues from a HCC patient undergoing hepatectomy in Beijing Cancer Hospital (52 Fucheng Road, Beijing) were also collected for TIF extraction. The tumor and nontumor tissues were confirmed by histopathologic examination. The information on these two patients is shown in Supporting Information Table S2. Human identifiers were removed to protect donor confidentiality. No antineoplastic therapy was given prior to surgery. The ethical and animal committees from the local institution approved the use of these samples. A small piece of mouse liver tissue or normal human liver tissue was stored in liquid nitrogen after resection. Remaining clinical specimens were sent to the laboratory on ice within 30 min. Another piece of each tissue was minced and used for hepatocyte separation based on the previously described method[14] and stored at −80 °C. The remainder of the tissue was used for TIF extraction. Liver subcellular organelles (mitochondria, plasma membrane) were separated using density gradient centrifugation[15] with modifications and stored at −80 °C.

TIF Collection. The TIF collection protocol was a modification of Celis' method.[12,13] Fresh tissues were cut into small pieces (1−3 mm^3) in PBS containing a protease inhibitor cocktail, transferred to 15-mL tubes, washed carefully with PBS, and immersed in an equal volume of PBS. Samples were incubated at 37 °C in a CO_2 incubator for different periods of time (0−8 h). The samples were then centrifuged at 1000*g* for 3 min and the supernatant was transferred to fresh Eppendorf tubes using a Paster pipet. Samples were further centrifuged at 2000*g* for 8 min and then at 20 000*g* for 30 min at 4 °C. After concentration in a vacuum dehydrator for 1 h, the TIF samples were snap-frozen in liquid nitrogen and stored at −80 °C in Eppendorf tubes. No additional freeze−thaw was carried out before use. The duration of storage before analysis was less than 1 year.

Two-Dimensional Differential In-Gel Electrophoresis (2D-DIGE) and Imaging. The pH of the sample was adjusted to 8.5 with 50 mM NaOH and the concentration was adjusted to 5 mg/mL with lysis buffer. Mouse liver TIF, hepatocyte lysate, and liver tissue lysate were labeled with Cy5, Cy3, and Cy2, respectively, using 400 pmol fluorochrome per 50 μg of protein. Labeling was performed for 30 min on ice in the dark. Reactions were then quenched by the addition of 1 μL of 10 mM lysine for 10 min on ice in the dark.

Fifty micrograms each of Cy2-, Cy3-, and Cy5-labeled samples were combined and an equal volume of 2× sample buffer (7 M urea, 2 M thiourea, 4% CHAPS, 1% Pharmalyte pH 3−10, and 20 mg/mL DTT) was added. The total volume of the sample was brought up to 410 μL with rehydration buffer (7 M urea, 2 M thiourea, 4% CHAPS, 0.5% Pharmalyte, and 10 mg/mL DTT). The sample was actively rehydrated into 24-cm 3−10 NL immobilized pH gradient (IPG) strips at 17 °C for 12 h using an IPGphor (GE Healthcare, Piscataway, NJ), followed by isoelectric focusing for a total of 80 kVh (ramp to 250 V in 30 min, hold at 1000 V for 1 h, ramp to 10 000 V in 5 h, hold at 10 000 V for 60 000 Vh). The IPG strips were equilibrated in equilibration buffer (6 M urea, 2% SDS, 50 mM Tris, pH 8.8, and 30% glycerol) supplemented with 0.5% DTT for 15 min at room temparature, followed by equilibration in 4.5% iodoacetamide in equilibration buffer for another 15-min incubation at room temprature. IPG stripes were placed on the top of homogeneous 12% polyacrylamide gels. Sodium dodecyl sulfate−polyacrylamide gel electrophoresis (SDS-PAGE) was carried out in the second dimension using Ettan DALT Six electrophoresis units (GE Healthcare, Piscataway, NJ).

After SDS-PAGE, gels were scanned on the Typhoon 9410 scanner (GE Healthcare, Piscataway, NJ) with Ettan DALT gel alignment guides using excitation/emission wavelengths specific for Cy2 (488 nm/520 nm), Cy3 (532 nm/580 nm), and Cy5 (633 nm /670 nm). The intensity was adjusted to ensure that the maximum pixel value of each image was within the range 60 000−90 000.

Western Blot. Proteins were electrophoresed on 12% polyacrylamide gels and then transferred to polyvinylidene fluoride membranes (Amersham Pharmacia Biotech, Uppsala, Sweden) using a trans-blot cell (Bio-Rad, Hercules, CA). After that, the membranes were incubated for 1 h at room temperature in TBST (20 mM Tris-HCl, 140 mM NaCl, pH 7.5, 0.05% Tween-20) containing 5% skim milk. Primary antibodies used were anti-GAPDH (glyceraldehyde-3-phosphate dehydrogenase) monoclonal antibody (diluted 1:1000, Kangcheng Biotechnology, Shanghai, China), anti-lamin B polyclonal antibody (diluted 1:1000, Santa Cruz, CA), anti-cyto C (cytochrome C) monoclonal antibody (diluted 1:1000, Neomarkers, Fremont, CA), anti-COX IV (cytochrome oxidase subunit IV) monoclonal antibody (diluted 1:1000, Molecular Probes, Eugene, OR), anti-flotillin-1 monoclonal antibody (diluted 1:500, BD, San Jose, CA), anti-beta-actin polyclonal antibody (diluted 1:500, Neomarkers, Fremont, CA). For each, membranes were incubated overnight at 4 °C, washed 3 times with TBST and incubated with horseradish peroxidase-conjugated secondary antibody (diluted 1:10 000, Santa Cruz, CA) for 1 h at room temperature. Visualization of the immunoreactive proteins was accomplished using enhanced chemiluminescence reagents (Pierce, Rockford, IL).

SDS-PAGE and In-Gel Digestion. Mouse liver TIF and hepatocyte lysate were separated by SDS-PAGE in 12% polyacrylamide gels. Normal human liver TIF was separated by SDS-PAGE in 12% and 8% polyacrylamide gels. TIFs from the HCC patient were separated by SDS-PAGE in 12% polyacrylamide gels. SDS-PAGE for each sample was run in duplicate for repeated mass spectrometry analysis. After staining with Coomassie Brilliant Blue, each gel was cut into 50 slices and destained with 25 mM ammonium bicarbonate/50% ACN. Gel particles were then dried completely by centrifugal lyophilization and digested with 0.01 μg/μL trypsin in 25 mM ammonium bicarbonate for 15 h at 37 °C. The supernatants were collected and the tryptic peptides were extracted from the gel sequentially with 5% TFA at 40 °C for 1 h and with 2.5% TFA50% ACN at 30 °C for 1 h. The extracts were pooled with the collected supernatants and dried completely by centrifugal lyophilization.

Protein Identification by Linear Ion Trap Mass Spectrometer (LTQ). The peptides were analyzed by reverse-phase (RP) HPLC-MS/MS using a Thermo Finnigan LTQ equipped with an electrospray ionization (ESI) source. The initial nano-LC run was performed on an LC-Packing system, which was configured with Famous, Swithos, and Ultimate, and controlled by Dionex chromatography software. Two RP C18 trap columns (C18 PepMap 100, 5 μm, 300-μm i.d. × 5 mm, Dionex Corporation, Sunnyvale, CA) were connected with a 10-port valve. When one column was being loaded, the other was used for separation. Peptides were eluted into the mass spectrometer (MS) through a PicoFrit tip column (BioBasicC18, 5 μm, 75-μm i.d. × 10 cm, 15-μm i.d. spray tip, New Objective, Woburn, MA) using an Ultimate pump. In this study, approximately 19 μL of peptide extract was injected into the trap column with the Famous loading pump at a flow rate of 10 μL/min under the UserProg injection mode. The adsorbed peptides were desalted on the trap column and eluted through the PicoFrit to the MS instrument by the Ultimate pump using a gradient of 2−40% buffer B (80% ACN and 0.1% TFA in water) in 90 min and 40−100% buffer B in 15 min. The LTQ-MS was operated in data-dependent mode using normalized collision energy of 35%. The temperature of the ion transfer tube was set at 200 °C and the spray voltage was set at 1.8 kV. The mass spectrometric analysis was performed with one full MS scan followed by five MS/MS scans on the five most intense ions from the MS spectrum with the dynamic exclusion settings of repeat count 1, repeat duration 30 s and exclusion duration 30 s. Searches were performed through a local Bioworks software (version 3.0) and allowed for acetyl (N-term), carbamidomethylation (C), oxidation (M) and maximum one missed trypsin cleavage. Peptide tolerance was 3 Da and MS/MS tolerance was 1 Da.

International Protein Index (IPI) mouse protein database (version 3.24, containing 52 326 entries, http://www.ebi.ac.uk/

IPI/) was downloaded as original database. The combined forward and reversed database was searched to assess the confidence of peptides identified. The false positive rate (FPR) for a given threshold score was calculated using following formula: FPR (%) = number of reversed peptide identifications/number of forward peptide identifications × 100%. The threshold score corresponding to FPR ≤ 5% was taken as cutoff for accepting individual MS/MS spectra (the cutoff scores were shown in Supporting Inforamtion Table S3). Proteins were assembled with those accepted peptides (≥2 unique peptides). If peptides match to multiple members of a protein family, the representative protein is selected according to a preference hierarchy of the IPI source databases (UniProtKB/Swiss-Prot, RefSeq, UniProtKB/TrEMBL, Ensembl). If there are two entries from the same database that both meet this criteria, the entry with the longest sequence is preferred.

Protein Identification by Quadrupole-Time-of-Flight (Q-TOF). Nanoscale RP-HPLC of the peptide mixture was carried out on a CapLC liquid chromatography system (Waters, Milford, MA). Peptide mixture was injected onto a precolumn (300 μm i.d. × 5 mm PepMap C18, 3 mm, LC Packings, Amsterdam, The Netherlands) for desalting. The separation was performed on a capillary C18 column (75 μm × 15 cm; LC Packings, Amsterdam, The Netherlands) by running a gradient of 4.5 min at 4% B (80% ACN, 0.1% formic acid), 65 min gradient to 50% B, 70 min gradient to 100% B, 73 min gradient to 4% B and 90 min at 4% B. Peptides were then directly eluted into a Q-TOF Micro mass spectrometer fitted with a nanoflow electrospray ion sourse (Micromass, Manchester, U.K.) at the flow rate of about 200 nL/min. The mass spectrometer was operated in positive ion mode with a source temperature of 80 °C and a spray voltage of 3000 V. Data-dependent analysis was employed (three most intense ions in each cycle): 1 s MS m/z 400−1500 and max 7.7 s MS/MS m/z 100−2000 (continuum mode), 50 s dynamic exclusion. Calibration was performed using glu-fib. The peak list files were generated with MassLynx 4.0 ProteinLynx (smooth 3/2 Savitzky Golay and center 4 channels/80% centroid). Then, the peak list files were used to search against the International Protein Index (IPI) human protein database (version 3.45, containing 71 983 entries, http://www.ebi.ac.uk/IPI/) through a local Mascot search engine server (version 2.1). Searches performed allowed for acetyl (N-term), carbamidomethylation (C), oxidation (M) and maximum 1 missed trypsin cleavage. Peptide tolerance and MS/MS tolerance were both 0.2 Da. The combined forward and reversed database was searched to assess the confidence of peptides identified. The FPR was calculated as mentioned above. The threshold score corresponding to FPR ≤ 5% was taken as cutoff for accepting individual MS/MS spectra (the cutoff scores were shown in Supporting Information Table S4). Proteins were assembled with those accepted peptides (≥2 unique peptides). If peptides match to multiple members of a protein family, the representative protein is selected according to a preference hierarchy of the IPI source databases (UniProtKB/Swiss-Prot, RefSeq, UniProtKB/TrEMBL, Ensembl). If there are two entries from the same database that both meet this criteria, the entry with the longest sequence is preferred.

Analysis of Liver TIF Proteins. Cellular component, biological process, and molecular function analyses of liver TIF proteins were based on Gene Ontology (GO) (http://www.geneontology.org/) with the aid of in-house software.[16] Mouse liver tissue data (7090 proteins, searched against the IPI mouse protein database, version 3.20) and mouse plasma data (4721 proteins, searched against the IPI mouse protein database, version 3.20) were used for comparison.[17] The appearance of each protein in mouse liver tissue, liver TIF, and plasma was counted.

Subtractive Analysis of TIFs from Human HCC Liver Tissues. TIF proteins of normal liver tissue from a hemangioma patient and paired tumor and nontumor liver tissues from an HCC patient were identified as described above. To increase confidence in proteins specifically expressed in tumor liver tissue, we applied a strict criterion whereby proteins identified in both nontumor liver TIF from HCC patient and normal liver TIF were subtracted. Only proteins uniquely identified in tumor liver TIF were retained.

Results

Evaluation of Cellular Contamination of TIF. Nuclear protein lamin B,[18,19] mitochondrial protein cyto C[20,21] or COX IV,[20−22] and plasma membrane protein flotillin-1[23,24] were used as organelle-specific markers for evaluation of contamination. We detected the expression levels of these proteins in hepatocyte lysate, liver perfusate, and TIF using mouse liver-organelle protein lysates as positive controls. All three organellar proteins could be detected in the corresponding positive controls and hepatocyte lysate, while none could be detected in TIF or liver perfusion (Figure 2A). Similar result was obtained in human liver TIF (Figure 2B). These results confirmed the absence of identifiable cellular protein contamination in TIF.

Interestingly, β-actin was represented by two bands in hepatocyte lysate; however, only the lower molecular-weight band was detected in TIF (Figure 2A). The same observation was made in human liver TIF (Figure 2B). In rat, the higher molecular-weight β-actin band appeared in TIF when liver tissue was incubated for 8 h (data not shown). This may due to the breakdown of rat liver cells after a long period of tissue incubation. Another commonly used protein loading control, GAPDH, was also detected in human liver samples (Figure 2B). Two GAPDH bands could be detected in TIF and liver tissue lysate, while only the higher molecular-weight band was detected in hepatocyte lysate and the intensity of this band was rather low. These results indicated the difference in protein quantity, and possibly modification/cleavage, intracellularly and in the hepatocyte extracellular space in the liver.

2D-DIGE Profiling of Liver TIF Proteome. To characterize the protein composition of liver TIF, we profiled the proteome of mouse liver TIF by 2D-DIGE. Surprisingly, the scattered distribution of liver TIF proteins (Figure 3, Cy5-labeled TIF proteins in red) did not display the "crowding" effect usually seen in the presence of high-abundance proteins. Given that the liver synthesizes 80% of plasma proteins, including albumin, this result was unexpected. Fortunately, however, the high-abundance proteins, which pose a significant problem in plasma proteome analysis, do not appear to pose a similar challenge in liver TIF analysis.

The mouse liver tissue (Cy2-labeled proteins in blue) and separated mouse hepatocytes (Cy3-labeled proteins in green) were co-electrophoresed with mouse liver TIF (Cy5-lableled proteins in red) by 2D-DIGE (Figure 3). As anticipated, liver tissue contains proteins from both hepatocytes (Figure 3B, merged images in cyan) and TIF (Figure 3C, merged images in magenta). However, the profiling pattern of liver TIF was distinctly different from that of hepatocytes; very few yellow spots appeared in the merged image (Figure 3D). In the next step, we analyzed the proteomes of mouse liver TIF and

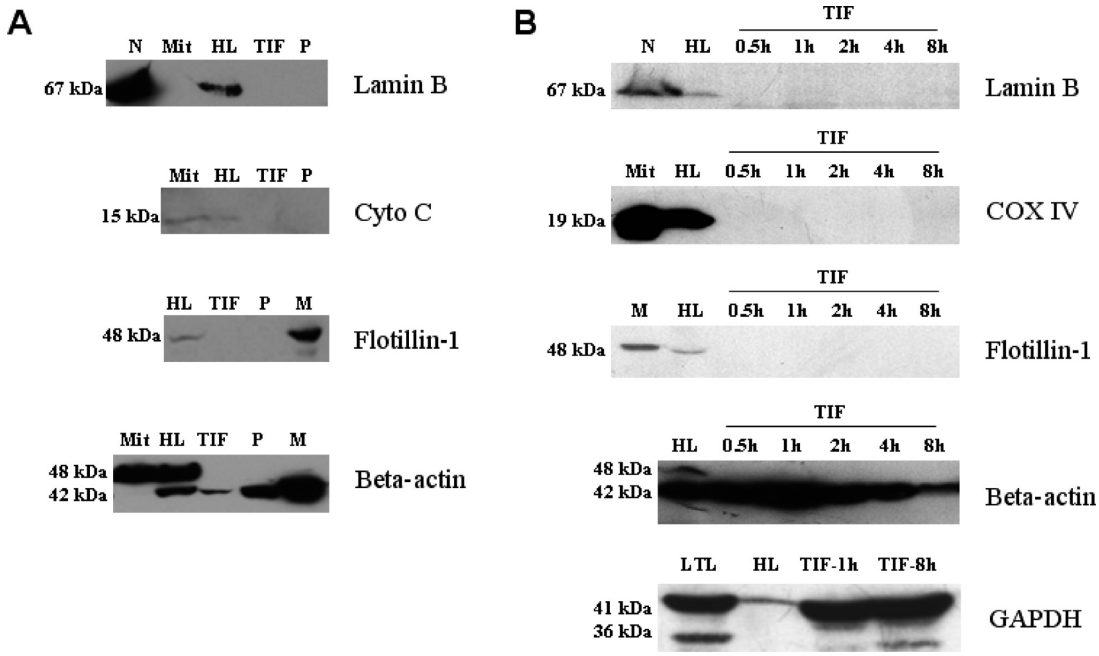

Figure 2. Western blot of nuclear protein lamin B, mitochondrial proteins cyto C or COX IV, and plasma membrane protein flotillin-1 for evaluation of contamination in (A) mouse liver TIF and (B) human liver TIF. HL, hepatocyte lysate; LTL, liver tissue lysate; P, perfusate; N, nuclear protein; Mit, mitochondrial protein; M, plasma membrane protein. Twenty-five micrograms of proteins was loaded in each lane. (A) Lamin B, cyto C, and flotillin-1 could be detected in the positive controls and the hepatocyte lysate, while none were detected in TIF or liver perfusate. Two β-actin bands were detected in mouse hepatocyte and only the lower band was detected in mouse TIF and perfusate. (B) Lamin B, COX IV, and flotillin-1 were detected in human hepatocyte lysate and TIFs extracted after 0.5−8 h incubation, using human liver subcellular organelle proteins as positive controls. All three subcellular organelle proteins could be detected in corresponding positive controls and hepatocyte lysate, while none were detected in TIFs collected from 0.5 to 8 h. As for mouse, two β-actin bands were detected in hepatocyte lysate, but only the lower band was detected in human TIF. The protein loading control GAPDH was also detected in human TIF, hepatocyte lysate, and liver tissue lysate. Two bands could be detected in TIF and liver tissue lysate, while only the higher molecular-weight band was seen in the hepatocyte lysate and the intensity of this band was rather low.

hepatocytes to determine the number of proteins shared by these two compartments.

Characterization of Liver TIF Proteins. 1. Molecular Weight and Isoelectric Point (p*I*) Distribution of TIF Proteins. Proteins in mouse liver TIF and hepatocytes were separated by SDS-PAGE. After mass spectrometric analysis and database searching, 1450 gene products were identified in mouse liver TIF and 1125 in mouse hepatocytes. Identified proteins are listed in Supporting Information Tables S5 and S6, together with accession number, molecular weight, p*I* value, coverage, and matched peptides with scores. The distribution of molecular weight and p*I* of mouse liver TIF proteins are shown in Figure 4. The molecular weights ranged from 3808 to 3 906 488 Da (Figure 4A). Most of the proteins were smaller than 100 kDa and predominantly (32%) in the range of 20−40 kDa. The p*I* values ranged from 3.76 to 11.78 (Figure 4B), with a valley around pH 7.4 and three peaks beside it; this pattern was similar to those of predicted proteomes of different organisms.[25] There was no particular bias in molecular weight or p*I* value distributions of mouse liver TIF proteins compared with common whole-organism proteomes. Considering the wide range of protein molecular weight and p*I* distribution and good protein solubility, TIF is a strong candidate to be a suitable material for proteomics analysis.

2. GO Annotation of Identified Proteins. Cellular components, enriched biological processes, and molecular functions of identified mouse liver TIF proteins are summarized in Figure 5 according to GO annotations. The TIF consisted of 27% nuclear proteins, 14% cytoskeleton proteins, 13% cytosolic proteins, 10% plasma membrane proteins, 8% endoplasmic reticulum proteins, 8% mitochondrial proteins, 7% extracellular matrix proteins, 4% Golgi apparatus proteins, 2% peroxisome proteins, 1% endosome proteins, 0.5% lysosome proteins, and 0.5% microtubule organizing center proteins. Exchange of materials between the cytoplasm and extracellular space is continuous and takes place through the endocytic and secretory pathways and shedding of membrane vesicles. Given this active protein exchange, the presence of proteins from the cytosol, endoplasmic reticulum, and plasma membrane in TIF can be justified. Proteins from the cytosol, cytoskeleton, endoplasmic reticulum, peroxisome, mitochondria, Golgi apparatus, endosome, and nucleus were significantly enriched compared to all the proteins encoded by the mouse genome ($P < 0.05$, based on hypergeometric distribution analysis[16]), indicating those organelles as the primary source of TIF proteins.

The enriched biological processes and molecular functions of these proteins are shown in Figure 5B,C. In addition to proteins involved in protein metabolism, biosynthesis, catabolism, and other common biological processes or functions, the identified gene products included proteins involved in protein transport, cytoskeleton organization and biogenesis, cell death, cell cycle, cell homeostasis, enzyme regulator activity, lipid binding, and antioxidant activity. The presence of these proteins in TIF is interesting because they may be involved in mediating the intercellular exchange of information through the TIF.

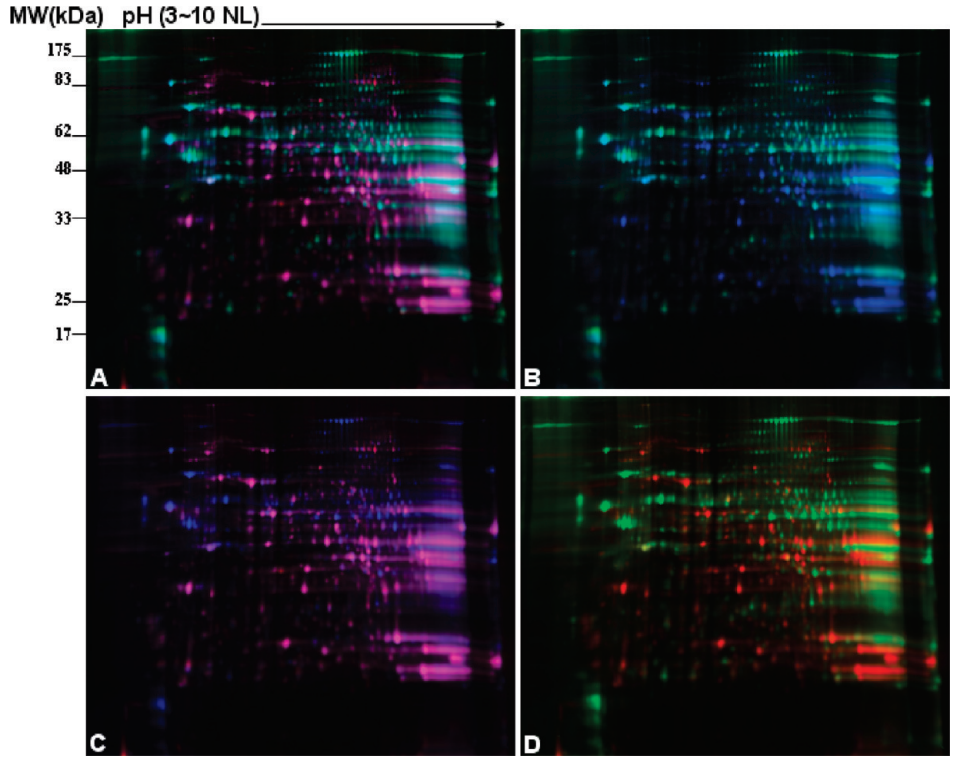

Figure 3. 2D-DIGE maps of proteins from mouse liver tissue (Cy2-labeled, blue), hepatocyte (Cy3-labeled, green), and TIF (Cy5-labeled, red). (A) Merged 2D-DIGE image of mouse liver tissue, hepatocyte, and TIF. (B) Merged image (cyan) of mouse liver tissue and hepatocyte. Hepatocyte proteins were included in liver tissue. (C) Merged image (magenta) of mouse liver tissue and TIF. TIF proteins were included in liver tissue. (D) Merged image (yellow) of mouse hepatocytes and TIF.

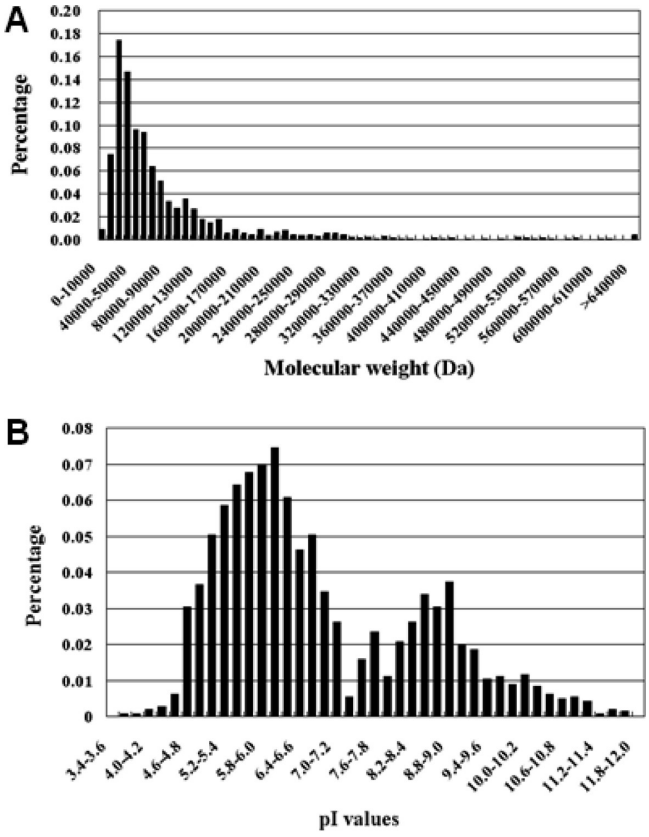

Figure 4. Molecular weight (A) and p*I* (B) distributions of proteins identified in mouse liver TIF.

3. Comparison with Mouse Liver and Plasma Proteome Data. Proteins identified in mouse liver tissue (7090 proteins), TIF (1450 proteins), hepatocytes (1125 proteins), and plasma (4721 proteins) were compared (Figure 6A). Only 299 proteins (21% of TIF proteins or 27% of hepatocyte proteins) were shared by mouse liver TIF and hepatocytes. The small degree of overlap between TIF and hepatocyte proteins was consistent with the result of DIGE analysis. Because the hepatocyte is a component of liver tissue, we integrated hepatocyte data with liver tissue data (Figure 6B). There were 1585 proteins shared by only liver and plasma, 785 proteins by only liver and TIF, 95 proteins by only plasma and TIF, and 282 proteins were identified in all three groups.

We assumed that there was a flow of protein from liver cells to the extracellular space and then to plasma and we have proposed four different protein-flow models for liver (Figure 6C). Model A presents those proteins which were expressed in liver tissue, secreted/shed into TIF, and then entered the plasma/blood. Regardless of the liver cell type that expressed them, proteins in model A are valuable candidates for biomarker discovery if they are dysregulated during the pathological process. Model B presents the liver proteins which could be secreted/shed into TIF but, for some reason, do not enter the bloodstream. Model C presents the liver proteins which do not enter TIF but could be found in plasma. It should be pointed out that those proteins might come from organs/tissues other than the liver. Model D presents the liver intracellular proteins which do not enter the TIF or the bloodstream. These are models, however, and the situation in reality is much more complex. For example, a protein not identified here may be absent from the sample or it may be present but unidentifiable

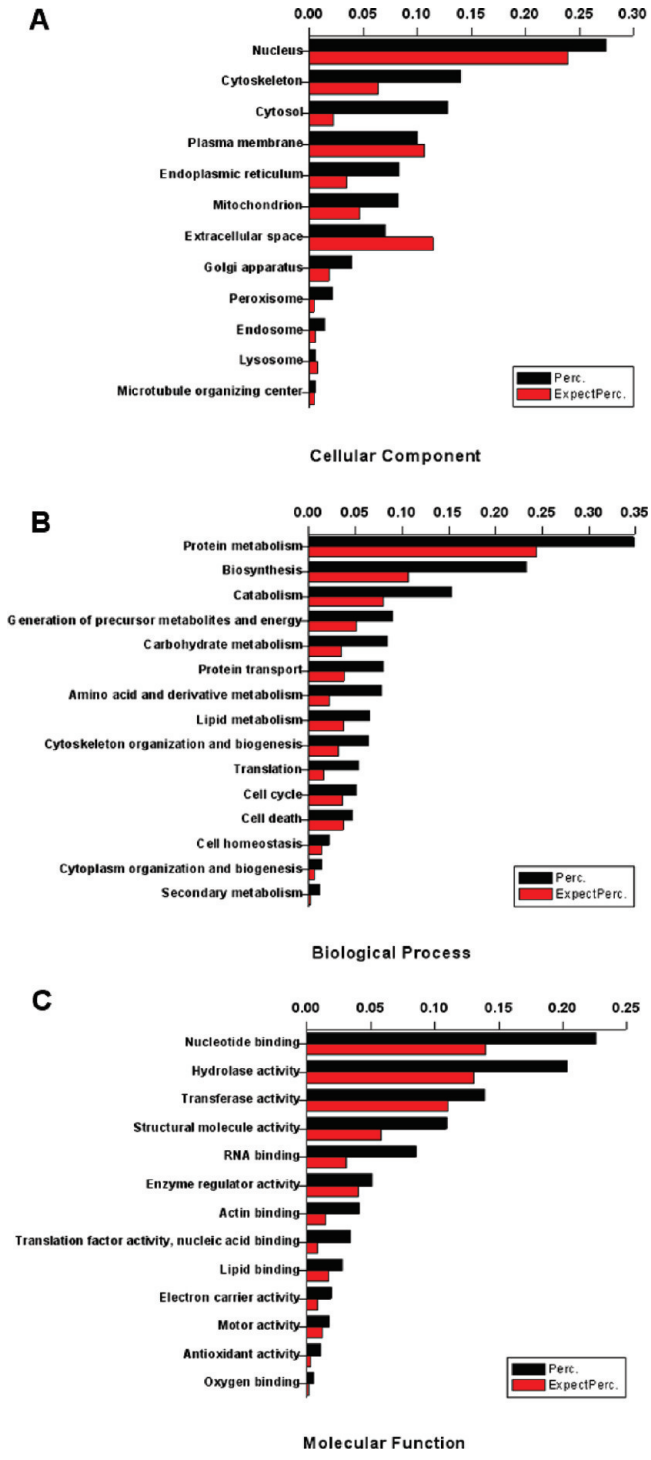

Figure 5. Cellular components (A), enriched biological processes (B), and molecular functions (C) of proteins identified in mouse liver TIF according to GO annotations. Black bar, percentage; red bar, expected percentage of all proteins encoded by mouse genome.

due to low abundance or limitations of the sensitivity of mass spectrometry.

Theoretically, proteins identified in liver tissue, TIF, and plasma are represented in model A (282 proteins, represented by YYY, with Y indicating that the protein was identified within each sample category). Proteins identified only in liver and TIF are presented in model B (785 proteins, represented by YYN, with N indicating that the protein was not identified in plasma).

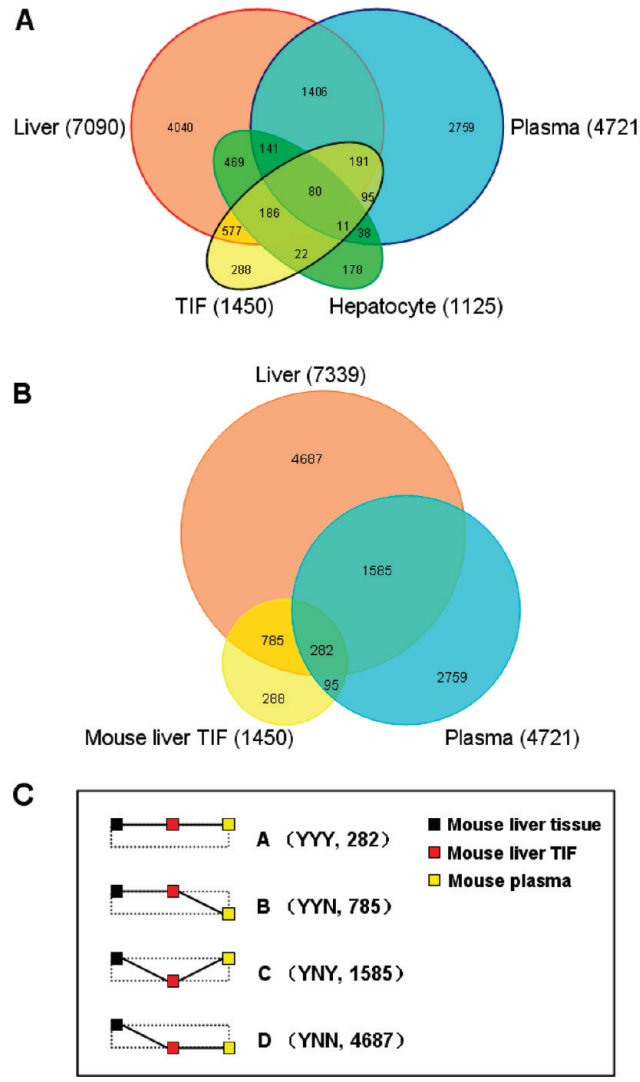

Figure 6. (A) Comparison of proteins identified in mouse liver tissue, mouse liver TIF, mouse hepatocytes, and mouse plasma. (B) Hepatocyte data were integrated into liver tissue data. There were 1585 proteins shared by only liver and plasma, 785 proteins by only liver and TIF, 95 proteins by only plasma and TIF, and 282 proteins could be identified in all three groups. (C) Four models of protein flow from liver cells to the extracellular space and then to plasma. Model A presents those proteins which were expressed in liver tissue, secreted/shed into TIF, and then entered the bloodstream (282 proteins, represented by YYY, Y indicates identified in that compartment). Model B presents the liver proteins which were secreted/shed into TIF but did not enter the bloodstream (785 proteins, represented by YYN, N indicates not identified). Model C presents the liver proteins that were not identified in TIF but could be found in plasma (1585 proteins, represented by YNY). Model D presents the liver intracellular proteins which did not enter TIF or the bloodstream/plasma (4687 proteins, represented by YNN).

Proteins identified in liver and plasma are shown in model C (1585 proteins, represented by YNY). Proteins identified only in liver were in model D (4687 proteins, represented by YNN) (Figure 6C). We used three sets of data to mimic the protein flow from liver cells to the extracellular space and plasma. Model A (YYY) corresponds to proteins flowing from liver to TIF and then to plasma; model B (YYN) corresponds to proteins flowing from liver cells to TIF; and model D (YNN) corresponds to proteins present only in liver tissue. GO annotation was

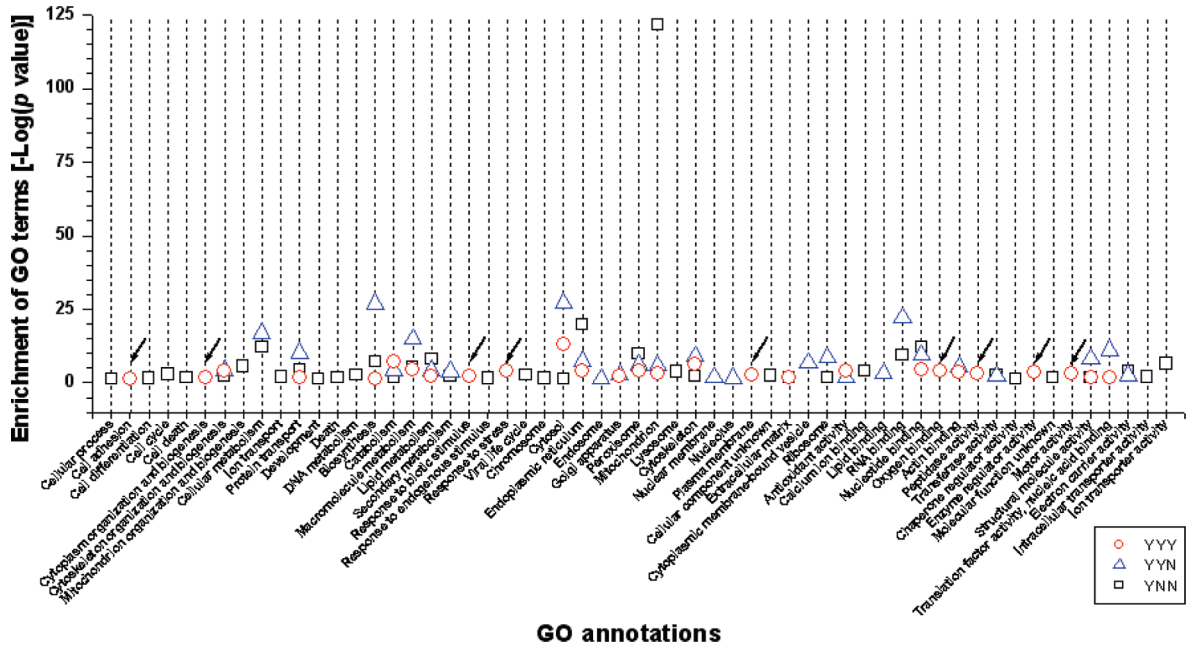

Figure 7. Significantly enriched GO annotations of mouse data from groups YNN, YYN and YYY. Proteins associated with cellular process, cell differentiation, cell cycle, cell death, mitochondrion organization and biogenesis, ion transport, development, death, DNA metabolism, response to endogenous stimulus, viral life cycle, chromosome, lysosome, cellular component unknown, calcium ion binding, chaperone regulator activity, molecular function unknown, intracellular transporter activity, and ion transporter activity were only enriched in the YNN group. Proteins associated with endosome, nuclear membrane, nucleolus, cytoplasmic membrane-bound vesicle, and lipid binding were only enriched in the YYN group, and proteins associated with cell adhesion, cytoplasm organization and biogenesis, response to biotic stimulus, response to stress, plasma membrane, oxygen binding, peptidase activity, enzyme regulator activity, and motor activity were enriched only in the YYY group (indicated by arrows).

performed to analyze the characteristics of proteins with different flow patterns. The significantly enriched GO annotations of these three sets of data are shown in Figure 7. It can be seen that proteins associated with cellular process, cell differentiation, cell cycle, cell death, mitochondrion organization and biogenesis, ion transport, development, death, DNA metabolism, response to endogenous stimulus, viral life cycle, chromosome, lysosome, cellular component unknown, calcium ion binding, chaperone regulator activity, molecular function unknown, intracellular transporter activity, and ion transporter activity were enriched only in the YNN group. Proteins associated with endosome, nuclear membrane, nucleolus, cytoplasmic membrane-bound vesicle, and lipid binding were enriched only in the YYN group, and proteins associated with cell adhesion, cytoplasm organization and biogenesis, response to biotic stimulus, response to stress, plasma membrane, oxygen binding, peptidase activity, enzyme regulator activity, and motor activity were enriched only in the YYY group (arrows in Figure 7). These results suggest that proteins associated with cell adhesion, cytoplasm organization and biogenesis, response to biotic stimulus, response to stress, plasma membrane, oxygen binding, peptidase activity, enzyme regulator activity, and motor activity are the major proteins released from liver to plasma and could serve as blood biomarkers of liver origin. Interestingly, the human liver TIF data, when compared to human liver proteome (HLP) data[26] (6788 proteins, searched against the IPI human protein database, version 3.07) and human plasma proteome (HPP) data[27] (3020 proteins, searched against the IPI human protein database, version 2.21), showed the specific enrichment of proteins associated with response to biotic stimulus, response to stress, extracellular space, and antioxidant activity in the YYY group (arrows in Supporting Information Figure S1). Both mouse and human data suggested that proteins associated with response to biotic stimulus and response to stress are blood proteins of liver origin.

Table 1. Subtractive Results of Liver TIFs from HCC Patient[a]

peptide counts of proteins identified in HCC TIF	number of unique proteins identified in HCC TIF	
	T versus *N*	*T* versus ($N + N_0$)
≥2	160	111
≥3	75	52
≥4	42	26
≥5	22	15
≥6	15	12

[a] *T*, TIF from HCC tumor tissue; *N*, TIF from nontumor liver tissue; N_0, TIF from normal human liver tissue.

Subtractive Analysis of Human HCC Liver TIFs. From the current Q-TOF data, we identified 325 gene products in normal human liver TIF (Supporting Information Table S7), 381 gene products in human HCC tumor TIF (Supporting Information Table S8), and 245 gene products in nontumor liver TIF (Supporting Information Table S9). We used this preliminary data to prepare a draft of the altered TIF proteome in HCC. A strict criterion was applied to identify with confidence proteins specifically expressed in HCC tumor. Proteins identified in both normal human liver TIF and nontumor TIF were subtracted and only unique proteins identified in tumor liver TIF were retained. As a result, we identified 111 unique proteins in tumor with ≥2 matched peptides or 12 unique proteins in tumor (Table 1); these 12 differentially expressed proteins were identified with high confidence, and had ≥6 matched peptides uniquely identified in tumor tissue. Further, 10 of these 12 proteins have been reported to be upregulated in HCC and other human cancers (Table 2).

Table 2. Unique Proteins Identified in HCC Tumor TIF with ≥6 Peptide Counts[a]

accession number	protein name	peptide counts ($T/N/N_0$)[b]	annotations
IPI00007752.1	Tubulin beta-2C chain	6/0/0	HCC[43]
IPI00022463.1	Serotransferrin precursor	6/0/0	/
IPI00216138.6	Transgelin	6/0/0	HCC (transgelin 2),[44] esophageal squamous cell carcinoma,[45] pancreatic ductal adenocarcinoma[46]
IPI00218976.1	Isoform C of Formimidoyltransferase-cyclodeaminase	6/0/0	HCC[47]
IPI00646304.4	peptidylprolyl isomerase B precursor	6/0/0	HCC (isomerase A),[48] HCV replication,[49] breast ductal carcinoma,[50] prostate cancer (isomerase Pin1)[51]
IPI00654875.1	Complement C4−B precursor	6/0/0	HCC,[52,53] lung cancer[54]
IPI00889156.1	IG kappa protein	6/0/0	HCC,[55] prostate cancer[55]
IPI00418471.6	Vimentin	7/0/0	HCC,[56] breast ductal carcinoma[57]
IPI00448925.3	IgG1 heavy chain protein (IGHG1)	7/0/0	HCC,[55] lung cancer[55]
IPI00479186.5	Isoform M2 of Pyruvate kinase isozymes M1/M2	7/0/0	HCC,[58] colon cancer,[59] renal carcinoma[60]
IPI00855785.1	Isoform 15 of Fibronectin precursor	7/0/0	HCC,[61,62] breast cancer,[63] prostatic cancer[64]
IPI00021439.1	Actin, cytoplasmic 1	12/0/0	/

[a] The 12 unique proteins shown in Table 1). [b] *T*, TIF from HCC tumor tissue; *N*, TIF from nontumor liver tissue; N_0, TIF from normal adult liver tissue.

Discussion

Proteomic analysis of TIF for pathology study was first carried out in innovative research done by Celis and coworkers. However, since then TIF has not been widely used in disease research. We are interested in applying this approach in liver disease research because liver synthesizes 80% of plasma proteins and the structure of the sinus hepaticus facilitates the release of disease-specific proteins into peripheral blood. In this preliminary study, we present the first characterization of the liver TIF proteome and evaluate its potential for application in biomarker discovery.

We extracted TIF from mouse liver and used traditional organelle marker proteins to confirm the absence of cellular protein contamination due to sample handling. All marker proteins were detected by Western analysis in positive controls and hepatocyte lysate but were absent from TIF. To minimize contamination due to cell breakage, we collected TIF extracted after 1 h of incubation.

2D-DIGE profiling of the TIF, hepatocyte, and liver tissue proteomes showed distinctive patterns of expression in TIF and hepatocytes. Western analysis of mouse and human β-actin and human GAPDH indicated differences between intra- and extracellular proteins in quantity and possibly post-translational modification/cleavage. Such changes may result in different biological functions for those isoforms. It has been reported that even the same protein may have different functions inside and outside the cell. For example, in addition to its intracellular functions, cAMP-dependent protein kinase (PKA) may well have an extracellular regulatory role in blood.[28]

In total, 1450 proteins involved in a variety of cell processes/functions were identified in mouse liver TIF after LTQ analysis and database searching,. Although only 141 signal transduction-associated proteins were identified, other potentially important factors, such as macrophage migration inhibitory factor (MIF), hepatoma-derived growth factor (HDGF), signal transducer and activator of transcription 3 (Stat3), were included. More sensitive techniques could be used in the future to detect key molecules occurring at low abundance.

We analyzed the distributions of molecular weight and p*I* of the TIF proteins and identified no particular bias in these parameters in the TIF proteome compared to other whole organism proteomes. On the basis of its high solubility and the absence of interfering high-abundance proteins, indicated by DIGE analysis, TIF appears to be a highly suitable material for proteomic analysis. TIF is amenable to analysis by standard gel-based and nongel-based approaches such as DIGE, cICAT, iTRAQ, SELDI, and MELDI.

The presence in TIF of proteins derived from cytosol, endoplasmic reticulum, plasma membrane, and other organelles might be due to endocytic and secretory action or shedding of membrane vesicles. For example, clathrin heavy chain, the major protein of the polyhedral coat of coated pits and vesicles, and AP-2 complex subunits, components of the adaptor complexes which link clathrin to receptors in coated vesicles, were detected in TIF. The shedding of membrane vesicles is an important way for normal and tumor cells to release proteins from the cell surface to the microenvironment.[29,30] Shed membrane vesicles participate in cell−matrix interactions,[31,32] tumor metastasis,[33] evasion of immune surveillance,[34] and may carry tumor markers that could be detected in the circulation of carcinoma patients.[35]

The relatively high proportion (27%) of TIF proteins of nuclear origin is puzzling because nuclear proteins should not be readily extracted by our TIF extraction protocol. Mouse plasma proteome data show that approximately 28% (710 proteins) of plasma proteins are of nuclear origin.[16] And in HPP data, approximately 12% (350 proteins) are nuclear proteins.[36] One possible explanation for these findings is the physiological release of cellular breakdown products into the circulation. However, the possible extracellular localization of those proteins should also be considered. For example, Jang and Shin found certain endoplasmic reticulum proteins located at the cell surface.[37,38]

Abundant plasma proteins such as albumin, ferritin, and hemoglobin were detected in TIF. Of TIF proteins, only 377 were included among the 4721 proteins of the mouse plasma proteome (Figure 6A), indicating more local proteins could be identified in TIF compared with plasma. Further, as indicated by the results of DIGE, TIF analysis is simplified by the absence of high-abundance proteins that compound proteomic analysis of plasma. The detection of critical regulatory molecules, such as signal transduction-associated proteins, suggests that TIF may be able to provide information on the molecular composition of the local microenvironment during pathopoiesis and also serve as a promising resource for biomarker discovery. Because the most promising biomarker candidates occur in body fluids, potential markers identified in TIF are more likely than those identified in tissues, to also be present in plasma.

The comparison of mouse TIF proteome data with mouse liver and plasma data suggested that proteins associated with cell adhesion, cytoplasm organization and biogenesis, response to biotic stimulus, response to stress, plasma membrane, oxygen binding, peptidase activity, enzyme regulator activity and motor activity are the major proteins which are released from liver to plasma and could serve as blood biomarkers of liver origin. The presence of proteins associated with response to biotic stimulus and response to stress were further supported by human data. For example, heat shock protein 27,[39] serum amyloid A protein,[40] and transforming growth factor $\beta 1$[41,42] are associated with response to biotic stimulus or response to stress and have been reported to be upregulated in the sera of HCC patients. This finding is significant for choosing clinical plasma validation candidates from differentially expressed tissue proteins, and may be helpful to biomarker studies starting from tissues.

The subtractive proteome analysis of paired tumor and nontumor human HCC liver TIFs demonstrates the high reliability of the data. Ten of the 12 differentially expressed proteins with ≥6 matched peptides identified in tumor TIF had been reported to be upregulated in HCC and other human cancers. This finding indicates the application potential for TIF in biomarker discovery, especially in solid tumors.

In this study, we extracted liver TIF and confirmed the absence of cellular protein contamination. For the first time, the characteristics of the liver TIF were analyzed using a proteomic approach and showed significant differences from the cellular proteome in profiling pattern, quantity, and possibly modification/cleavage of proteins. The protein composition of liver TIF reflects the physiological and pathological state of the tissue and offers more information and a higher local protein concentration than plasma. Without interference from high-abundance proteins and protein elements from other tissues and organs, TIF represents a promising source for biomarker discovery. Our study showed the potential of liver TIF for application in liver disease biomarker discovery and provided basic data for further study in human and mouse. Despite these early advances, much remains to be done in analysis of liver TIF. In the next step, quantitative proteomic techniques will be applied to analyze clinical samples and further our understanding of the molecular mechanisms underlying HCC development and progression.

Acknowledgment. We thank Dr. Julio E. Celis for the constructive discussion with him about the extraction protocol. Also thank Drs. Yunwei Hao, Lihai Guo, Ping Wan, Yuanbiao Guo, and Xinyu Deng for their help and advice. This work was partially supported by Chinese State High-tech Program (2006AA02A308), Chinese State Key Projects for Basic Research (2006CB910401, 2006CB910801, and 2006CB910600, 2010CB912700 and 2006CB503910), National Natural Science Foundation of China (30700988, 30700356, 30972909), Chinese State Key Project Specialized for Infectious Diseases (2008ZX10002-016, 2009ZX10004-103, 2009ZX09301-002), International Scientific Collaboration Program (2009DFB33070, 2008GR0763) and grant from State Key Laboratory of Proteomics (SKLP-K200805).

Supporting Information Available: Supplemental Figure 1 shows the GO annotations of comparison among human liver TIF, liver tissue and plasma proteome data. Supplemental Table 1 shows the comparison between TIF and plasma/serum for their application in disease proteomics. Supplemental Table 2 shows the clinical information of patients. Supplemental Table 3 shows the cutoff scores of mouse liver data from LTQ. Supplemental Table 4 shows the cutoff scores of human liver TIF data from Q-TOF. Supplemental Table 5 shows the proteins identified in mouse liver TIF. Supplemental Table 6 shows the proteins identified in mouse hepatocyte. Supplemental Table 7 shows the proteins identified in normal adult liver TIF. Supplemental Table 8 shows the proteins identified in HCC tumorous liver TIF. Supplemental Table 9 shows the proteins identified in HCC nontumorous liver TIF. This material is available free of charge via the Internet at http://pubs.acs.org.

References

(1) Jungermann, K.; Katz, N. Functional specialization of different hepatocyte populations. *Physiol. Rev.* **1989**, *69* (3), 708–64.
(2) Drucker, C.; Parzefall, W.; Teufelhofer, O.; Grusch, M.; Ellinger, A.; Schulte-Hermann, R.; Grasl-Kraupp, B. Non-parenchymal liver cells support the growth advantage in the first stages of hepatocarcinogenesis. *Carcinogenesis* **2006**, *27* (1), 152–61.
(3) Liotta, L. A.; Kohn, E. C. The microenvironment of the tumour-host interface. *Nature* **2001**, *411* (6835), 375–9.
(4) Hanash, S. Integrated global profiling of cancer. *Nat. Rev. Cancer* **2004**, *4* (8), 638–44.
(5) Mueller, M. M.; Fusenig, N. E. Friends or foes—bipolar effects of the tumour stroma in cancer. *Nat. Rev. Cancer* **2004**, *4* (11), 839–49.
(6) Fidler, I. J. The pathogenesis of cancer metastasis: the 'seed and soil' hypothesis revisited. *Nat. Rev. Cancer* **2003**, *3* (6), 453–8.
(7) Coussens, L. M.; Werb, Z. Inflammation and cancer. *Nature* **2002**, *420* (6917), 860–7.
(8) Sedlaczek, P.; Frydecka, I.; Gabrys, M.; Van Dalen, A.; Einarsson, R.; Harlozinska, A. Comparative analysis of CA125, tissue polypeptide specific antigen, and soluble interleukin-2 receptor alpha levels in sera, cyst, and ascitic fluids from patients with ovarian carcinoma. *Cancer* **2002**, *95* (9), 1886–93.
(9) Rosty, C.; Christa, L.; Kuzdzal, S.; Baldwin, W. M.; Zahurak, M. L.; Carnot, F.; Chan, D. W.; Canto, M.; Lillemoe, K. D.; Cameron, J. L.; Yeo, C. J.; Hruban, R. H.; Goggins, M. Identification of hepatocarcinoma-intestine-pancreas/pancreatitis-associated protein I as a biomarker for pancreatic ductal adenocarcinoma by protein biochip technology. *Cancer Res.* **2002**, *62* (6), 1868–75.
(10) Anderson, N. L.; Polanski, M.; Pieper, R.; Gatlin, T.; Tirumalai, R. S.; Conrads, T. P.; Veenstra, T. D.; Adkins, J. N.; Pounds, J. G.; Fagan, R.; Lobley, A. The human plasma proteome: a nonredundant list developed by combination of four separate sources. *Mol. Cell. Proteomics* **2004**, *3* (4), 311–26.
(11) Faca, V. M.; Song, K. S.; Wang, H.; Zhang, Q.; Krasnoselsky, A. L.; Newcomb, L. F.; Plentz, R. R.; Gurumurthy, S.; Redston, M. S.; Pitteri, S. J.; Pereira-Faca, S. R.; Ireton, R. C.; Katayama, H.; Glukhova, V.; Phanstiel, D.; Brenner, D. E.; Anderson, M. A.; Misek, D.; Scholler, N.; Urban, N. D.; Barnett, M. J.; Edelstein, C.; Goodman, G. E.; Thornquist, M. D.; McIntosh, M. W.; DePinho, R. A.; Bardeesy, N.; Hanash, S. M. A mouse to human search for plasma proteome changes associated with pancreatic tumor development. *PLoS Med.* **2008**, *5* (6), e123.
(12) Celis, J. E.; Gromov, P.; Cabezon, T.; Moreira, J. M.; Ambartsumian, N.; Sandelin, K.; Rank, F.; Gromova, I. Proteomic characterization of the interstitial fluid perfusing the breast tumor microenvironment: a novel resource for biomarker and therapeutic target discovery. *Mol. Cell. Proteomics* **2004**, *3* (4), 327–44.
(13) Celis, J. E.; Moreira, J. M.; Cabezon, T.; Gromov, P.; Friis, E.; Rank, F.; Gromova, I. Identification of extracellular and intracellular signaling components of the mammary adipose tissue and its interstitial fluid in high risk breast cancer patients: toward dissecting the molecular circuitry of epithelial-adipocyte stromal cell interactions. *Mol. Cell. Proteomics* **2005**, *4* (4), 492–522.
(14) Berry, M. N.; Friend, D. S. High-yield preparation of isolated rat liver parenchymal cells: a biochemical and fine structural study. *J. Cell Biol.* **1969**, *43* (3), 506–20.
(15) Fleischer, S.; Kervina, M. Subcellular fractionation of rat liver. *Methods Enzymol.* **1974**, *31* (Pt A), 6–41.
(16) Li, D.; Li, J.; Ouyang, S.; Wu, S.; Wang, J.; Xu, X.; Zhu, Y.; He, F. An integrated strategy for functional analysis in large-scale proteomic research by gene ontology. *Prog. Biochem. Biophys.* **2005**, *32* (11), 1026–9.

(17) Lai, K. K.; Kolippakkam, D.; Beretta, L. Comprehensive and quantitative proteome profiling of the mouse liver and plasma. *Hepatology* **2008**, *47* (3), 1043–51.
(18) Pendas, A. M.; Zhou, Z.; Cadinanos, J.; Freije, J. M.; Wang, J.; Hultenby, K.; Astudillo, A.; Wernerson, A.; Rodriguez, F.; Tryggvason, K.; Lopez-Otin, C. Defective prelamin A processing and muscular and adipocyte alterations in Zmpste24 metalloproteinase-deficient mice. *Nat. Genet.* **2002**, *31* (1), 94–9.
(19) Kosak, S. T.; Skok, J. A.; Medina, K. L.; Riblet, R.; Le Beau, M. M.; Fisher, A. G.; Singh, H. Subnuclear compartmentalization of immunoglobulin loci during lymphocyte development. *Science* **2002**, *296* (5565), 158–62.
(20) Mootha, V. K.; Bunkenborg, J.; Olsen, J. V.; Hjerrild, M.; Wisniewski, J. R.; Stahl, E.; Bolouri, M. S.; Ray, H. N.; Sihag, S.; Kamal, M.; Patterson, N.; Lander, E. S.; Mann, M. Integrated analysis of protein composition, tissue diversity, and gene regulation in mouse mitochondria. *Cell* **2003**, *115* (5), 629–40.
(21) Da Cruz, S.; Xenarios, I.; Langridge, J.; Vilbois, F.; Parone, P. A.; Martinou, J. C. Proteomic analysis of the mouse liver mitochondrial inner membrane. *J. Biol. Chem.* **2003**, *278* (42), 41566–71.
(22) Taylor, S. W.; Fahy, E.; Zhang, B.; Glenn, G. M.; Warnock, D. E.; Wiley, S.; Murphy, A. N.; Gaucher, S. P.; Capaldi, R. A.; Gibson, B. W.; Ghosh, S. S. Characterization of the human heart mitochondrial proteome. *Nat. Biotechnol.* **2003**, *21* (3), 281–6.
(23) Nebl, T.; Pestonjamasp, K. N.; Leszyk, J. D.; Crowley, J. L.; Oh, S. W.; Luna, E. J. Proteomic analysis of a detergent-resistant membrane skeleton from neutrophil plasma membranes. *J. Biol. Chem.* **2002**, *277* (45), 43399–409.
(24) Bae, T. J.; Kim, M. S.; Kim, J. W.; Kim, B. W.; Choo, H. J.; Lee, J. W.; Kim, K. B.; Lee, C. S.; Kim, J. H.; Chang, S. Y.; Kang, C. Y.; Lee, S. W.; Ko, Y. G. Lipid raft proteome reveals ATP synthase complex in the cell surface. *Proteomics* **2004**, *4* (11), 3536–48.
(25) Wu, S.; Wan, P.; Li, J.; Li, D.; Zhu, Y.; He, F. Multi-modality of pI distribution in whole proteome. *Proteomics* **2006**, *6* (2), 449–55.
(26) Jiang, Y.; Ying, W.; Wu, S.; Chen, M.; Guan, W.; Yang, D.; Song, Y.; Liu, X.; Li, J.; Hao, Y.; Sun, A.; Geng, C.; Li, H.; Mi, W.; Zhang, Y.; Zhang, J.; Chen, X.; Li, L.; Gong, Y.; Li, T.; Ma, J.; Li, D.; Yuan, X.; Zhang, X.; Xue, X.; Zhu, Y.; Qian, X.; He, F.; Zhong, F.; Shen, H.; Lin, C.; Lu, H.; Wei, L.; Cao, J.; Yun, D.; Gao, M.; Fan, H.; Cheng, G.; Yu, Y.; Xie, L.; Wang, H.; Yang, P. Y.; Shi, L.; Tong, W.; Li, X.; Wang, Y.; Liu, S.; Sheng, Q.; Zeng, R.; Sun, Y.; Xu, Y.; Cai, J.; He, P.; Gao, H.; Zhao, X. H.; Tan, Y.; Yan, H.; Yang, Y.; Huang, J.; Han, Z. G.; He, Q.; Chen, P.; Liang, S.; Zhao, M.; Mao, X.; Yu, H.; Cao, Z.; Li, Y.; Dai, W.; Jiang, H.; Wang, D.; Zheng, J.; Xue, G.; Tang, Y.; Cheng, J.; Liu, Y.; Wang, X.; Jia, J.; An, D.; Wang, Z.; Li, Q.; Cui, T. First insight into the human liver proteome from PROTEOME^{SKY}-LIVER^{Hu} 1.0, a publicly available database. *J. Proteome Res.* **2010**, *9* (1), 79–94.
(27) Omenn, G. S.; States, D. J.; Adamski, M.; Blackwell, T. W.; Menon, R.; Hermjakob, H.; Apweiler, R.; Haab, B. B.; Simpson, R. J.; Eddes, J. S.; Kapp, E. A.; Moritz, R. L.; Chan, D. W.; Rai, A. J.; Admon, A.; Aebersold, R.; Eng, J.; Hancock, W. S.; Hefta, S. A.; Meyer, H.; Paik, Y. K.; Yoo, J. S.; Ping, P.; Pounds, J.; Adkins, J.; Qian, X.; Wang, R.; Wasinger, V.; Wu, C. Y.; Zhao, X.; Zeng, R.; Archakov, A.; Tsugita, A.; Beer, I.; Pandey, A.; Pisano, M.; Andrews, P.; Tammen, H.; Speicher, D. W.; Hanash, S. M. Overview of the HUPO Plasma Proteome Project: results from the pilot phase with 35 collaborating laboratories and multiple analytical groups, generating a core dataset of 3020 proteins and a publicly-available database. *Proteomics* **2005**, *5* (13), 3226–45.
(28) Shaltiel, S.; Schvartz, I.; Korc-Grodzicki, B.; Kreizman, T. Evidence for an extra-cellular function for protein kinase A. *Mol. Cell. Biochem.* **1993**, *127*−*128*, 283–91.
(29) De Broe, M. E.; Wieme, R. J.; Logghe, G. N.; Roels, F. Spontaneous shedding of plasma membrane fragments by human cells in vivo and in vitro. *Clin. Chim. Acta* **1977**, *81* (3), 237–45.
(30) Taylor, D. D.; Black, P. H. Shedding of plasma membrane fragments. Neoplastic and developmental importance. *Dev. Biol.* **1986**, *3*, 33–57.
(31) Dolo, V.; Ginestra, A.; Cassara, D.; Violini, S.; Lucania, G.; Torrisi, M. R.; Nagase, H.; Canevari, S.; Pavan, A.; Vittorelli, M. L. Selective localization of matrix metalloproteinase 9, beta1 integrins, and human lymphocyte antigen class I molecules on membrane vesicles shed by 8701-BC breast carcinoma cells. *Cancer Res.* **1998**, *58* (19), 4468–74.
(32) Dolo, V.; D'Ascenzo, S.; Violini, S.; Pompucci, L.; Festuccia, C.; Ginestra, A.; Vittorelli, M. L.; Canevari, S.; Pavan, A. Matrix-degrading proteinases are shed in membrane vesicles by ovarian cancer cells in vivo and in vitro. *Clin. Exp. Metastasis* **1999**, *17* (2), 131–40.
(33) Dolo, V.; Ginestra, A.; Ghersi, G.; Nagase, H.; Vittorelli, M. L. Human breast carcinoma cells cultured in the presence of serum shed membrane vesicles rich in gelatinolytic activities. *J. Submicrosc. Cytol. Pathol.* **1994**, *26* (2), 173–80.
(34) Taylor, D. D.; Black, P. H. Inhibition of macrophage Ia antigen expression by shed plasma membrane vesicles from metastatic murine melanoma lines. *J. Natl. Cancer Inst.* **1985**, *74* (4), 859–67.
(35) Dolo, V.; Adobati, E.; Canevari, S.; Picone, M. A.; Vittorelli, M. L. Membrane vesicles shed into the extracellular medium by human breast carcinoma cells carry tumor-associated surface antigens. *Clin. Exp. Metastasis* **1995**, *13* (4), 277–86.
(36) Ping, P.; Vondriska, T. M.; Creighton, C. J.; Gandhi, T. K.; Yang, Z.; Menon, R.; Kwon, M. S.; Cho, S. Y.; Drwal, G.; Kellmann, M.; Peri, S.; Suresh, S.; Gronborg, M.; Molina, H.; Chaerkady, R.; Rekha, B.; Shet, A. S.; Gerszten, R. E.; Wu, H.; Raftery, M.; Wasinger, V.; Schulz-Knappe, P.; Hanash, S. M.; Paik, Y. K.; Hancock, W. S.; States, D. J.; Omenn, G. S.; Pandey, A. A functional annotation of subproteomes in human plasma. *Proteomics* **2005**, *5* (13), 3506–19.
(37) Shin, B. K.; Wang, H.; Yim, A. M.; Le Naour, F.; Brichory, F.; Jang, J. H.; Zhao, R.; Puravs, E.; Tra, J.; Michael, C. W.; Misek, D. E.; Hanash, S. M. Global profiling of the cell surface proteome of cancer cells uncovers an abundance of proteins with chaperone function. *J. Biol. Chem.* **2003**, *278* (9), 7607–16.
(38) Jang, J. H.; Hanash, S. Profiling of the cell surface proteome. *Proteomics* **2003**, *3* (10), 1947–54.
(39) Feng, J. T.; Liu, Y. K.; Song, H. Y.; Dai, Z.; Qin, L. X.; Almofti, M. R.; Fang, C. Y.; Lu, H. J.; Yang, P. Y.; Tang, Z. Y. Heat-shock protein 27: a potential biomarker for hepatocellular carcinoma identified by serum proteome analysis. *Proteomics* **2005**, *5* (17), 4581–8.
(40) He, Q. Y.; Zhu, R.; Lei, T.; Ng, M. Y.; Luk, J. M.; Sham, P.; Lau, G. K.; Chiu, J. F. Toward the proteomic identification of biomarkers for the prediction of HBV related hepatocellular carcinoma. *J. Cell Biochem.* **2008**, *103* (3), 740–52.
(41) Sacco, R.; Leuci, D.; Tortorella, C.; Fiore, G.; Marinosci, F.; Schiraldi, O.; Antonaci, S. Transforming growth factor beta1 and soluble Fas serum levels in hepatocellular carcinoma. *Cytokine* **2000**, *12* (6), 811–4.
(42) Song, B. C.; Chung, Y. H.; Kim, J. A.; Choi, W. B.; Suh, D. D.; Pyo, S. I.; Shin, J. W.; Lee, H. C.; Lee, Y. S.; Suh, D. J. Transforming growth factor-beta1 as a useful serologic marker of small hepatocellular carcinoma. *Cancer* **2002**, *94* (1), 175–80.
(43) Tang, J.; Niu, J. W.; Xu, D. H.; Li, Z. X.; Li, Q. F.; Chen, J. A. Alteration of nuclear matrix-intermediate filament system and differential expression of nuclear matrix proteins during human hepatocarcinoma cell differentiation. *World J. Gastroenterol.* **2007**, *13* (20), 2791–7.
(44) Shi, Y. Y.; Wang, H. C.; Yin, Y. H.; Sun, W. S.; Li, Y.; Zhang, C. Q.; Wang, Y.; Wang, S.; Chen, W. F. Identification and analysis of tumour-associated antigens in hepatocellular carcinoma. *Br. J. Cancer* **2005**, *92* (5), 929–34.
(45) Qi, Y.; Chiu, J. F.; Wang, L.; Kwong, D. L.; He, Q. Y. Comparative proteomic analysis of esophageal squamous cell carcinoma. *Proteomics* **2005**, *5* (11), 2960–71.
(46) Sitek, B.; Luttges, J.; Marcus, K.; Kloppel, G.; Schmiegel, W.; Meyer, H. E.; Hahn, S. A.; Stuhler, K. Application of fluorescence difference gel electrophoresis saturation labelling for the analysis of microdissected precursor lesions of pancreatic ductal adenocarcinoma. *Proteomics* **2005**, *5* (10), 2665–79.
(47) Sun, W.; Xing, B.; Sun, Y.; Du, X.; Lu, M.; Hao, C.; Lu, Z.; Mi, W.; Wu, S.; Wei, H.; Gao, X.; Zhu, Y.; Jiang, Y.; Qian, X.; He, F. Proteome analysis of hepatocellular carcinoma by two-dimensional difference gel electrophoresis: novel protein markers in hepatocellular carcinoma tissues. *Mol. Cell. Proteomics* **2007**, *6* (10), 1798–808.
(48) Lim, S. O.; Park, S. J.; Kim, W.; Park, S. G.; Kim, H. J.; Kim, Y. I.; Sohn, T. S.; Noh, J. H.; Jung, G. Proteome analysis of hepatocellular carcinoma. *Biochem. Biophys. Res. Commun.* **2002**, *291* (4), 1031–7.
(49) Watashi, K.; Ishii, N.; Hijikata, M.; Inoue, D.; Murata, T.; Miyanari, Y.; Shimotohno, K. Cyclophilin B is a functional regulator of hepatitis C virus RNA polymerase. *Mol. Cell* **2005**, *19* (1), 111–22.
(50) Bini, L.; Magi, B.; Marzocchi, B.; Arcuri, F.; Tripodi, S.; Cintorino, M.; Sanchez, J. C.; Frutiger, S.; Hughes, G.; Pallini, V.; Hochstrasser, D. F.; Tosi, P. Protein expression profiles in human breast ductal carcinoma and histologically normal tissue. *Electrophoresis* **1997**, *18* (15), 2832–41.
(51) Ryo, A.; Uemura, H.; Ishiguro, H.; Saitoh, T.; Yamaguchi, A.; Perrem, K.; Kubota, Y.; Lu, K. P.; Aoki, I. Stable suppression of tumorigenicity by Pin1-targeted RNA interference in prostate cancer. *Clin. Cancer Res.* **2005**, *11* (20), 7523–31.

(52) Takezaki, E.; Murakami, S.; Nishibayashi, H.; Kagawa, K.; Ohmori, H. [A clinical study of complements as a marker of a hepatocellular carcinoma]. *Gan No Rinsho* **1990**, *36* (12), 2119–22.
(53) Tsai, J. F.; Tsai, J. H.; Chang, W. Y. Relationship of serum alpha-fetoprotein to circulating immune complexes and complements in patients with hepatitis B surface antigen-positive hepatocellular carcinoma. *Gastroenterol. Jpn.* **1990**, *25* (3), 388–93.
(54) Gminski, J.; Mykala-Ciesla, J.; Machalski, M.; Drozdz, M.; Najda, J. Immunoglobulins and complement components levels in patients with lung cancer. *Rom. J. Intern. Med.* **1992**, *30* (1), 39–44.
(55) Chen, Z.; Gu, J. Immunoglobulin G expression in carcinomas and cancer cell lines. *FASEB J.* **2007**, *21* (11), 2931–8.
(56) Hu, L.; Lau, S. H.; Tzang, C. H.; Wen, J. M.; Wang, W.; Xie, D.; Huang, M.; Wang, Y.; Wu, M. C.; Huang, J. F.; Zeng, W. F.; Sham, J. S.; Yang, M.; Guan, X. Y. Association of Vimentin overexpression and hepatocellular carcinoma metastasis. *Oncogene* **2004**, *23* (1), 298–302.
(57) Chahed, K.; Kabbage, M.; Ehret-Sabatier, L.; Lemaitre-Guillier, C.; Remadi, S.; Hoebeke, J.; Chouchane, L. Expression of fibrinogen E-fragment and fibrin E-fragment is inhibited in the human infiltrating ductal carcinoma of the breast: the two-dimensional electrophoresis and MALDI-TOF-mass spectrometry analyses. *Int. J. Oncol.* **2005**, *27* (5), 1425–31.
(58) Taketa, K.; Shimamura, J.; Ueda, M.; Shimada, Y.; Kosaka, K. Profiles of carbohydrate-metabolizing enzymes in human hepatocellular carcinomas and preneoplastic livers. *Cancer Res.* **1988**, *48* (2), 467–74.
(59) Eigenbrodt, E.; Basenau, D.; Holthusen, S.; Mazurek, S.; Fischer, G. Quantification of tumor type M2 pyruvate kinase (Tu M2-PK) in human carcinomas. *Anticancer Res.* **1997**, *17* (4B), 3153–6.
(60) Oremek, G. M.; Teigelkamp, S.; Kramer, W.; Eigenbrodt, E.; Usadel, K. H. The pyruvate kinase isoenzyme tumor M2 (Tu M2-PK) as a tumor marker for renal carcinoma. *Anticancer Res.* **1999**, *19* (4A), 2599–601.
(61) Torbenson, M.; Wang, J.; Choti, M.; Ashfaq, R.; Maitra, A.; Wilentz, R. E.; Boitnott, J. Hepatocellular carcinomas show abnormal expression of fibronectin protein. *Mod. Pathol.* **2002**, *15* (8), 826–30.
(62) Matsui, S.; Takahashi, T.; Oyanagi, Y.; Takahashi, S.; Boku, S.; Takahashi, K.; Furukawa, K.; Arai, F.; Asakura, H. Expression, localization and alternative splicing pattern of fibronectin messenger RNA in fibrotic human liver and hepatocellular carcinoma. *J. Hepatol.* **1997**, *27* (5), 843–53.
(63) Suer, S.; Baloglu, H.; Gungor, Z.; Sonmez, H.; Kokoglu, E. The distribution of tissue fibronectin and sialic acid in human breast cancer. *Cancer Biochem. Biophys.* **1998**, *16* (1−2), 63–70.
(64) Suer, S.; Sonmez, H.; Karaaslan, I.; Baloglu, H.; Kokoglu, E. Tissue sialic acid and fibronectin levels in human prostatic cancer. *Cancer Lett.* **1996**, *99* (2), 135–7.

PR9009172